Structural Coloration in *Caloenas Nicobarica* Pigeons and Refractive Index Modulated Sensing

*Ijaz Rashid, Muhammad Umair Hassan, Abbas Khandwalla, Rayan Mohammed Ameen, Ali Kemal Yetisen, Qing Dai, and Haider Butt**

The Nicobar pigeon (*Caloenas Nicobarica*) belongs to the extinct dodo-bird family and has been declared as an endangered species. Here, microscopic and spectroscopic measurements are carried out on the bird's feathers to study the structural coloration originating from the barbule nanostructures. A range of color shades is recorded with changing viewing and illumination angles at different locations of the feathers. A spectacular variation in colors is generated by photonic structures; red, green, and blue and their blends are observed. Hydrophobicity of the optical material is also investigated. A contact angle of ≈156° is observed demonstrating it to be superhydrophobic. Experimental observations of the optical properties are analyzed on these feathers for sensing made possible due to the material and structural properties at the interface between barbule's surface and solution. An optical response is observed with a redshift in optical spectra with increasing refractive index of the solution, which is correlated with concentration values. The structural coloration in Nicobar pigeon can be adopted for many practical applications such as color selective filters, nonreflecting coatings, and refractive index-based sensing.

1. Introduction

The earliest recorded study of iridescence of birds' feathers is found in Robert Hooke's book Micrographia (1665),[1] in which he researched on Peacock feathers and discovered the effect of color changes in different refractive index media. However, birds are not the only species which possess these colors; – insects,[2–12] marine life,[13–18] and plants[19–24] also exhibit pure structural coloration beside some examples combining structural colorations with colorants or pigments.[25] Morpho butterflies,[10] beetles,[11] and dragonflies[12] show iridescent coloration purely due to their complex structural nanoscale features on their wings and bodies. Irish moss also possesses layered structure in its cuticles, where organization and dimensions of lamellae are responsible for its blue color.[17] Bragg gratings and multilayer reflectors are responsible for vivid colors of marine crustaceans.[15] Anhydrous guanine-based biogenic photonic crystal plates have been reported to be found in fish and spiders.[18] Additionally, the pointillist appearance of blue *Pollia* fruit is because of its multilayer stacks of cells.[23] Such structural coloration in nature has evolved to provide Batesian mimicry, camouflage, conspecific recognition, predation, signal communication, and mating behavior.

Many species of birds show structural colors.[26–33] Multiple optical processes can also be simultaneously present in one species.[34] Combination of these different optical processes complements each other to generate brilliant colors. Optical effects occur mainly because of photonic structures including thin films,[35] multilayer Bragg reflectors,[26] diffraction gratings.[36] The iridescent coloration of specula of ducks is because of the single 2D hexagonal lattice of melanosomes as well as thin film of keratin.[30] Feathers of hummingbirds exhibit brilliant color because of optical periodic pallets containing layered air gaps.[37] Investigation of structural coloration and underlying nanoscale architecture has led to many practical applications through adopting modern synthetic routes and nanofabrication techniques to bioinspired replication of nanophotonic structures.[38–44] Their application s include self-cleaning surfaces,[42] color-selective filters,[44] and antireflective coatings,[45] sensors,[46] supercapacitors,[47] fabrics,[48] tough materials,[49] and art.[50]

Nicobar pigeon (*Caloenas Nicobarica*) is an iridescent near-threatened bird species in the family of pigeons or doves.[31] Nicobar pigeons inhabit Nicobar islands of Malay Archipelago, Solomons, Palu, and south-eastern coastal regions of India,

I. Rashid, Dr. M. U. Hassan, A. Khandwalla, Dr. H. Butt
School of Engineering
University of Birmingham
Edgbaston, Birmingham B15 2TT, UK
E-mail: h.butt@bham.ac.uk
Dr. R. M. Ameen
Department of Metallurgy and Material Science
University of Birmingham
Edgbaston, Birmingham B15 2TT, UK
Dr. A. K. Yetisen
School of Chemical Engineering
University of Birmingham
Edgbaston, Birmingham B15 2TT, UK
Prof. Q. Dai
Nanophotonics Research Division
CAS Center for Excellence in Nanoscience
National Center for Nanoscience and Technology
Beijing 100190, China

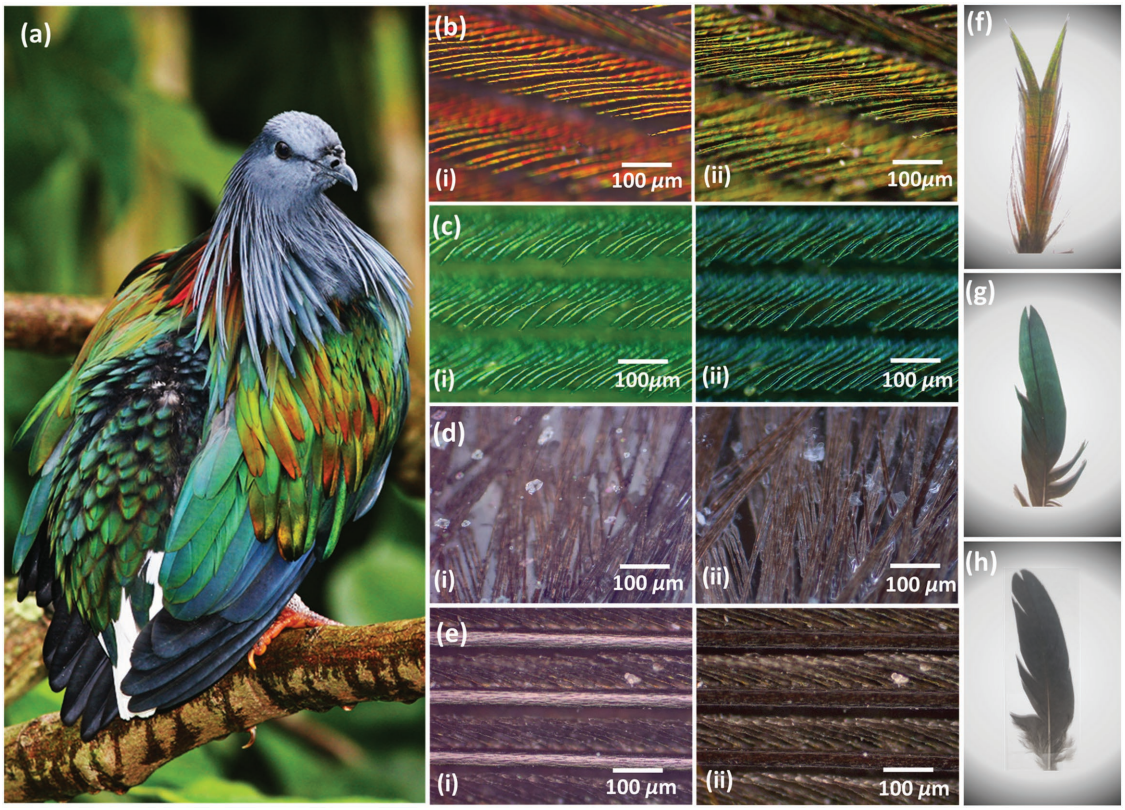

Figure 1. a) The Nicobar pigeon. b) The bright-field (BF) and dark-field (DF) microscopic images of a red-green (RG) feather showing the color shift from red (i) to green (ii), respectively. c) The BF and DF microscopic images of a green-blue (GB) feather showing the color shift from green (i) to blue (ii), respectively. d,e) BF and DF microscopic images were taken at different locations from the bottom of a GB feather showing no optical effects. No optical effects were observed in all kinds of feathers when viewed from the bottom. f,g) Photographic images taken from the top of an RG and GB feather. h) Photographic image taken from the bottom of a GB feather. All feathers appeared dark gray when viewed from the bottom.

and its population has been decreasing due to lowland deforestations.[27] The bird's feathers exhibit all colors (blue, green, red) across the visible spectrum (**Figure 1**a). Surprisingly, color mechanism/photonic effects of the Nicobar pigeon has not reported. In this work, we use optical, microscopic, and spectroscopic techniques to study the structural coloration in Nicobar pigeon. With an incident broadband light, bird's barbule diffracted highly intense colors (red, green, blue), which undergo a systematic shift at an angle of ≈45°. Feathers showed low transmittance and hardly allowed light to pass though indicating high absorption across a wide range of the incident wavelengths. We rule out the consideration that low transmittance across the entire visible range can be due to the high reflectance from the feather top surface, as reflectance occurs only for selective wavelengths recorded in reflection experiments as discussed in the following discussion. We used laser-induced far-field diffraction to reconstruct the microscopic landscape and arrangement of barbules in the vane of the feather. Super-hydrophobicity nature of Nicobar's feathers showed a large contact angle of ≈156°, comparable to those of in the duck family.[29] In our recent work, we reported on advanced electrochemical and optical techniques for quantitative sensing.[46,51–53] In the present work, we exploit interfacial and geometric properties of the naturally structured feathers for refractive index sensing.

2. Results and Discussion

The difference between both microscopic schemes enabled imaging the feather from the same eyepiece location while they were subject to normal and oblique illumination angles, respectively (Figure S1, Supporting Information). The vane of the red–green (RG) and green–blue (GB) feather exhibited a blueshift from red to green and green to blue when viewing mode was shifted from the bright field to the dark field (Figure 1b,c). The downy barbs and afterfeathers are dark gray and do not exhibit any structural coloration or photonic effect. The downy barbs and afterfeathers were random and no particular arrangement/order was perceived at these locations for both types of feather. The bottom side of both feathers was also dark and exhibited no color or change in color when viewed through either in bright field (BF) or dark field (DF) modes (Figure 1f,g). In the transmission mode, light was highly absorbed by the feather and yielded no patterns or optical effects across the whole length and breadth of the feather. Photographs of whole RG and GB feathers are shown from the top and GB feather from the bottom in Figure 1f–h, respectively. In general, the barbules and hooklets attached with barbs (in the vane section) were responsible for iridescent colors and photonic effects. Barbs, rachis, or shaft did not exhibit photonic effects.

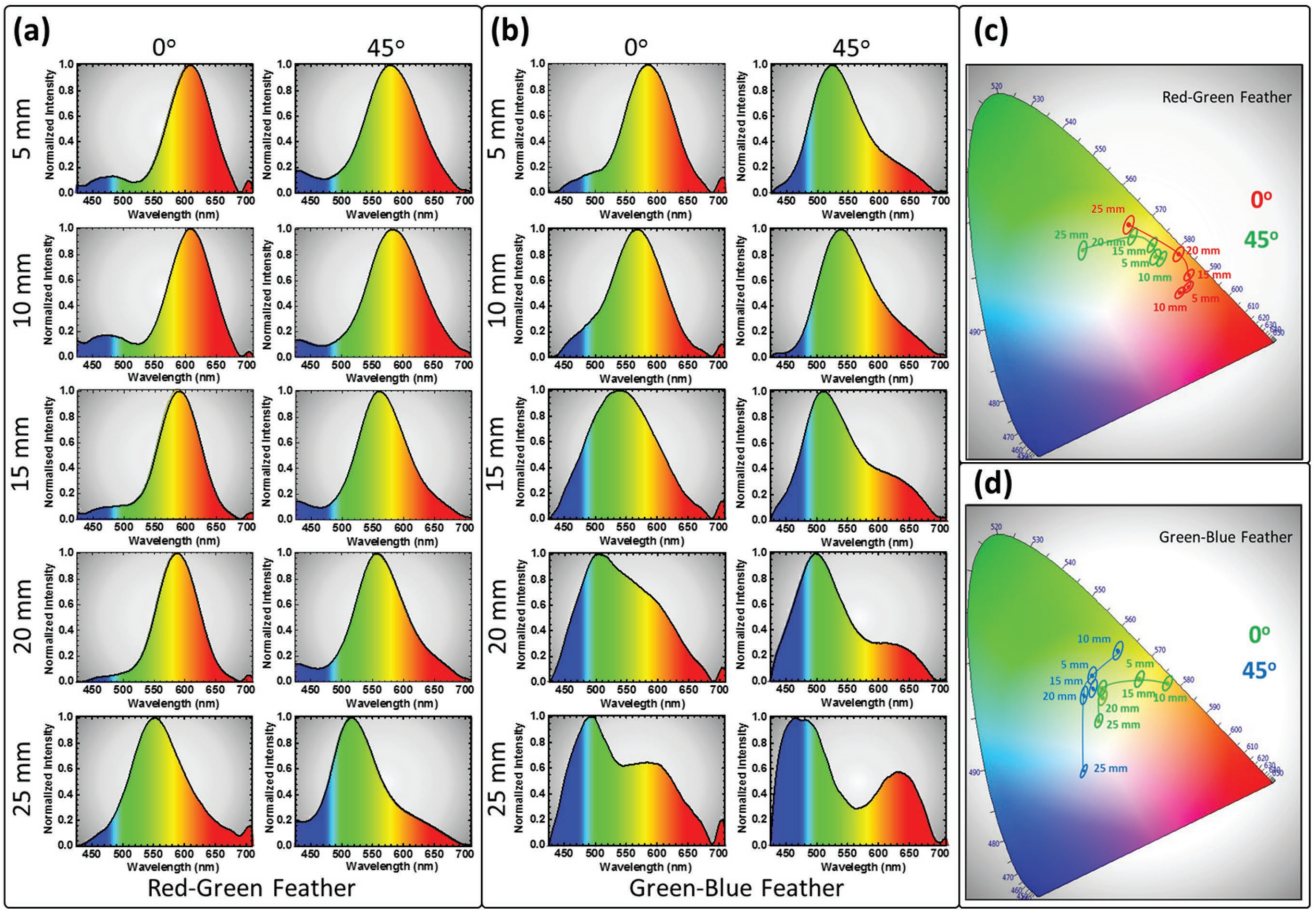

Figure 2. Optical spectra of a) RG and b) GB feathers at different locations, while feathers are illuminated at 0° and 45°, respectively. c,d) The illumination angle at 0° and 45° shifted the spectra from red to green and green to blue for RG and GB feather, respectively. CIE images indicating the visible shift of colors upon switching the incidence angle from 0° to 45° at different equidistant locations on RG and GB feathers, respectively.

Optical diffraction from different points at RG and GR feathers were recorded at normal to the feather plane with 0° and 45° illumination angles. A broadband light source was used for the illumination and feathers were moved horizontally by means of a translational stage. Spectra were recorded with 5 mm increments (**Figure 2**). The spectra for RG (GB) feather blueshifted, from longer wavelengths of red (or green) to shorter wavelengths of green (or blue), as the angle of measurement, increased from 0° to 45°. In both feathers, moving from the point closer to the tip (5 mm) toward the hollow shaft (25 mm) shifted the diffracted light to shorter wavelengths. To perceive the color, all recorded diffraction curves were plotted according to Commission Internationale de l'éclairage (CIE) standards. The perceived colors and their shift with translation on the RG and GB feathers are highlighted in Figure 2c,d, respectively.

A change in the viewing elevation angle shifted the overall peak, while the broadband light was incident from the normal, whereas, rotation of feathers along vertical-axis (azimuthal angle) showed only the change in overall intensity of particular color as viewed from certain elevation and, in general, did not shift the colors. In a rotation setup to characterize the feathers, the broadband light was illuminated from the normal (top) and optical spectra were recorded between normal to 45° with an increment of 5°, while feather was rotated between 0° and 90° on a stage (**Figure 3**a). Measurements in Figure 3b,c were taken from the mid-section for both feathers, where the color was the most brilliant. The spot size of the broadband light was ≈2 mm. For RG (GB) feather, elevation-dependent recording of colors showed a shift from 600 nm (yellow) to 550 nm (green), while viewing angle was moved from normal 0° to oblique 45°. For the z-axis rotation (azimuthal angle), measurements were carried out at 0° and 45° elevation angles. The azimuthal angle variation was resulted solely intensity changes between a maximum of ≈600 nm (550 nm) and a minimum 550 nm (500 nm) for RG (GB) feathers and showed no shift in the peak values of the wavelength (Figure 3). Therefore, one of the repercussions of the change in the azimuth was that both feathers appeared dark at certain angles and bright at others – no detectable diffraction was observed at certain illumination and viewing settings.

Observers viewing from different locations perceive colors of Nicobar pigeon differently. Two interchangeable broadband light sources were used to illuminate the samples at 0° and 45° with respect to the normal defining the illumination plane (**Figure 4**). A diffused tungsten light source illuminated the

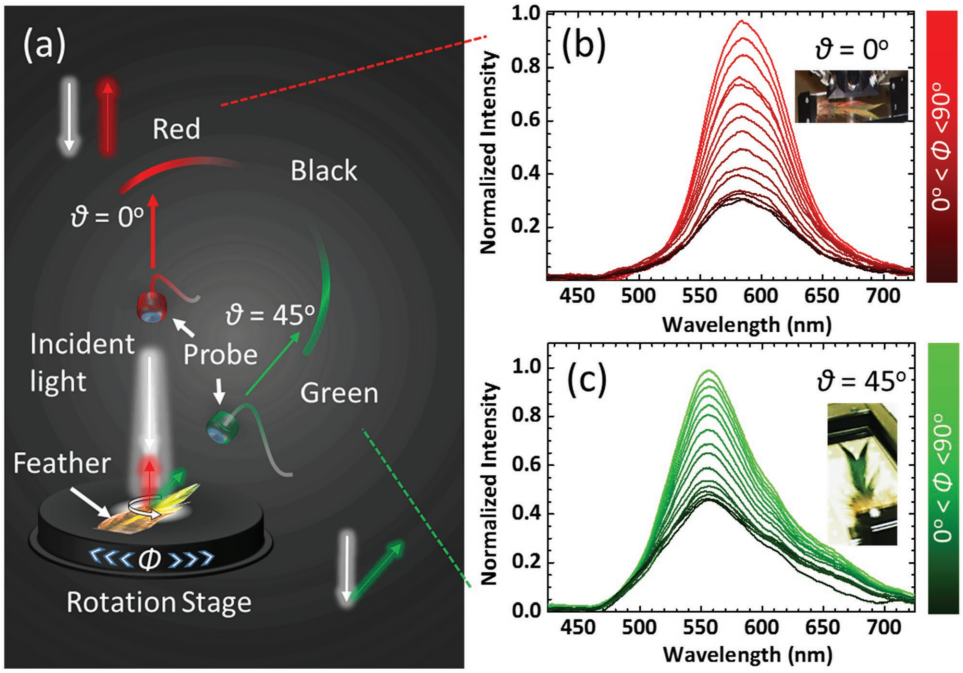

Figure 3. Optical characterization of the feathers. a) Schematic for rotational measurement setup. b,c) Variation in optical intensities at $\theta = 0°$ and 45°, while Φ was rotated through 0°–90°.

whole feather and, a fiber optic source illuminated the feathers from a small ≈1 cm circular spot. Photographs were then taken at 0° and 45° in the recording plane. At 0° (45°) of recording for the RG feather, the spot exhibited predominant red (to green) color, whereas surrounding part of the feather irradiated green (and red) color. Similarly, 0° (45°) of recording for the GB feather, the spot showed green (to blue) color, whereas surrounding part reflected blue (to green) color. Hence, both the illumination angle and different viewing positions define the perceived color.

There is a distinction between our selected RG and GB feathers in terms of their mechanical and optical properties. The RG feather is a neck (capital) feather which is softer than the BG wing (humeral) feather – a generic feature of all birds. **Figure 5**a–l provides magnified microscopic images of the Nicobar pigeon feathers. Beside optical response to the broadband light, melanosomes might also play a part in coloration. Investigation of the RG feather revealed rich coloration, especially close to the main shaft, and other locations in the vane. Each barbule consisted of several segments that showed a spectacular range of colors in the visible spectrum. Basic colors including red, green, and blue were observed. These colors can be observed in one barbule alone, where red, green, and blue can be seen in adjacent segments. However, the change in hue within these segments are not merely the pigments that are strictly localized in well-defined segments in the barbule but are coupled with photonic effects at different tilt angles, which are responsible for the vivid show of the range of colors at certain angles (Figure 5). The variation in relative structural orientation in adjacent segments of single barbule results in color change. The selected BG wing feather was hard and almost all barbules along the vane showed identical optical behavior. When viewed under the microscope, the straight horizontal part of barbules provided a light-blue color and became green along the curved part, the curve angle being almost 45°. Under high magnification the color of the barbule on either side of the main shaft was different, the upper being green and the lower being blue, showing the difference in the effective viewing angles (Figure 5i,l). The difference in colors was due to curves (change in angle) present in barbules.

The most dominant coloration mechanism in bird feathers is due to multilayer films.[8,26,28,54] Similarly, the pigeon and dove family of birds have multilayer structures in their barbules.[32,33,55] We suggest that barbules of Nicobar pigeon possess a multilayer photonic structure, in which transparent keratin film encapsulates air-filled multilayered melanosome cavities – the tilt in the illumination or/and observation angle result in the change in the brightness and shift in colors. In the investigation of the Nicobar pigeon feathers, the peaks of the spectra shifted to shorter wavelengths with an increase in the angle of incidence. Additionally, at larger angles of incidence, the diffraction amplitude decreased considerably – complete blackening below the spectrometer sensitivity was observed at certain angles. The differences in refractive indices of the structured layers and their spatial periodicity, as well as the relative thickness of barbules, play a key role in determining which wavelengths are coherently backscattered. One of the main characteristics of structural iridescent feathers is that the color varies depending on the angle between illumination and observation as well as between the feather orientation and the plane of examination. The change in the thickness of layers and thereby characteristic of photonic structures within the layers dictate the incident light to travel shorter or longer distances through the layers with increasing or decreasing angle with the

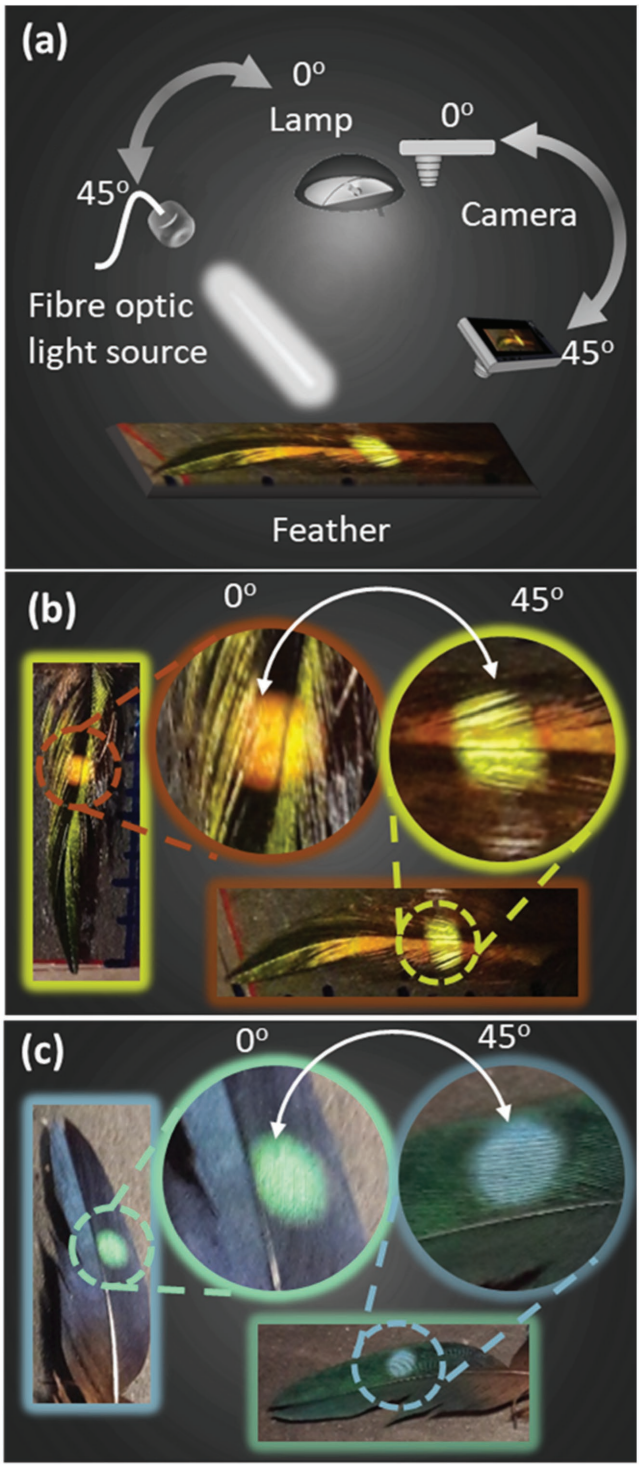

Figure 4. Angle-dependent characterization of the feathers. a) Schematic of two-source illumination of the feathers using two interchangeable light sources: a diffused incandescent tungsten lamp and a collimated broadband light to observe two colors at same viewing angle simultaneously. b,c) Photographs of RG and GB feathers taken from two different angles.

barbule plane, respectively. The backscattered coherent light changes its color according to the direction of the reflection (Figure 5m). These observations are consistent with the barb behaving as a set of multilayer Bragg mirrors. See Figure S2 (Supporting Information) for transmission experiments in the far-field setup carried out to observe the light transmission and diffraction behavior of the feathers in the transmission mode.

Nicobar feathers exhibited superhydrophobic characteristics. A contact angle of 156° was measured at the colored part of the vane of a GB feather (**Figure 6**). When the tilt angle was changed from 0° to 90°, the droplet (1 μL) remained clung to the feather surface. The feather was rotated in a way that the horizontal component of gravity pulled the droplet in opposite to the growth direction of the feather. Figure 6c shows different droplet sizes sprinkled over the feather, where superhydrophobic nature of the feather kept all droplets in stationary and spherical shapes. The dark part of the feather, the afterfeather, also exhibited hydrophobicity, where two droplets have been shown to retain a large contact angle at colored vane and afterfeather regions of the feather of the Nicobar pigeon (Figure 6d). Notice that in the afterfeather the barbs and barbules have no particular distribution and are placed randomly, their random distribution does not deteriorate the hydrophobic properties. The Nicobar Islands experience heavy rainfall (up to 3800 mm per year), especially in the monsoon season, the superhydrophobic properties of the Nicobar pigeon's feathers explain the natural selection necessary for the bird's survival in such climatic conditions.

Micro- or nanoscale surface texturing has been used to enhance the hydrophobic properties of the range of different materials. Naturally occurring texturing is ubiquitous and present in the animal and plant kingdom. We used scanning electron microscopy (SEM) to analyze the surface of the barbules (Figure 6e–h). The feather was Au coated (thickness ≈10 nm) using DC sputtering, before loading into in the SEM to prevent the charging effect. The barbule density in the mid-section of the vane had a value of ≈170 mm^{-1}; and therefore, the interspacing between the adjacent barbules was ≈6 μm. SEM images revealed a nonsmooth surface with protruded parts of keratin. In magnified SEM images, a long-range 1D periodic structure was also observed. The 1D structure resembled a grating and exhibited a duty cycle of ≈1000 mm^{-1}, having a feature size of 100 nm (Figure 6h). These structure spanned over the length of the segment within the barbule.

We demonstrate an RG feather-based sensor that shows a linear response over a large range of refractive index values. Although the feather is superhydrophobic, the interfacial and geometric properties can be exploited to sense the change in the refractive index of the liquid media by pouring it directly on the top of the feather and measuring the colorimetric response. For sensing experiments, deionized water and different glucose concentrations ranging between 10 and 200 × 10^{-3} M were utilized (**Figure 7**). Dark-field optical microscopy with a spectrophotometer fixed at the objective was used to record the spectra for concentration measurements. The feather was placed under the optical microscope and the reference images (and related spectra) were taken in the dark field. The sensing zone was selected close to the end point of the main shaft, where optical effects were the strongest. After selecting the sensing zone, droplets with increasing glucose concentration were carefully poured using a micropipette. For each concentration, optical spectra were recorded and the droplet was removed from the

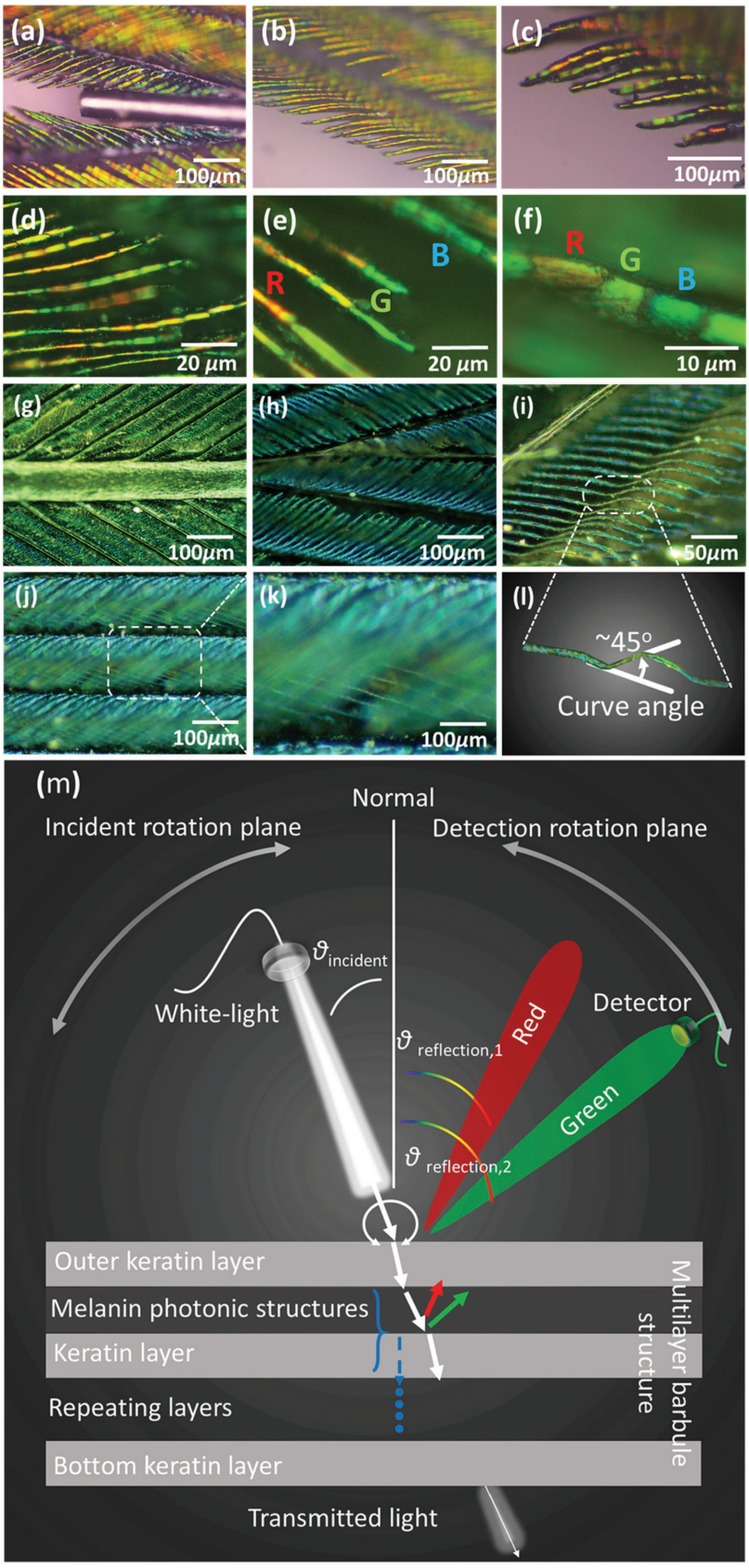

feather using a microsuction syringe. The wavelength initially redshifted with DI water, followed by the positive trend with increasing glucose concentration; and thereby to an increasing refractive index. The underlying mechanism of sensing is due to the focusing properties of the curved droplet poured on the feather. The long wavelength initially diffracting at a large angle without a droplet now bends toward the normal of the feather plane. The increasing refractive index due to increasing glucose concentration guides the longer wavelengths more toward the objective lens, resulting in the observed redshift. The initial sensor response was large (sensitivity ≈0.28 nm/× 10^{-3} M) and linear for concentrations between 0 and 50 × 10^{-3} M, which tends to flatten for higher concentrations. The response (sensitivity ≈0.03 nm/× 10^{-3} M) saturated at 80–200 × 10^{-3} M glucose concentration.

3. Conclusions

We studied color plumage of Nicobar pigeon (*Caloenas Nicobarica*) using spectroscopy and angle-resolved measurements. The iridescence of colors was linked with the photonic structures coupled with melanosome layered structures in barbules. The feathers exhibited wavelength-selective diffraction of light at certain illumination/observation angles. These feathers also showed different colors when observed and probed at different locations on the feather, resulting in a rainbow-like behavior. We also carried out contact angle experiments to assess the feathers' response against water. Superhydrophobic properties were measured resulting in a large contact angle of ≈156°. We also used the optical response of these feathers for refractive index sensing. Due to the interfacial and geometrical properties at the interface between feather surface and solution, a redshift

Figure 5. Mechanism of structural coloration in Nicobar pigeon feathers. a–f) Microscopic images of predominant RG feather showing a range of colors spanning the whole visible spectrum at some selected locations of the feather, where each segment possessed different colors. g–l) Microscopic images of GB feather showing two dominant colors. In a single GB feather, angle resolution was the clearest, where tilt in the feather resulted in two different colors. Internal structural features were assumed to be different in each segment of the RG feather. The internal structural profile was supposed to be more uniform that persisted almost all along the feather. Therefore, only two colors were visible because of the curve at almost midpoint of the feathers. m) Schematic of the proposed color-selective diffraction mechanism from a barbule structure of the feather.

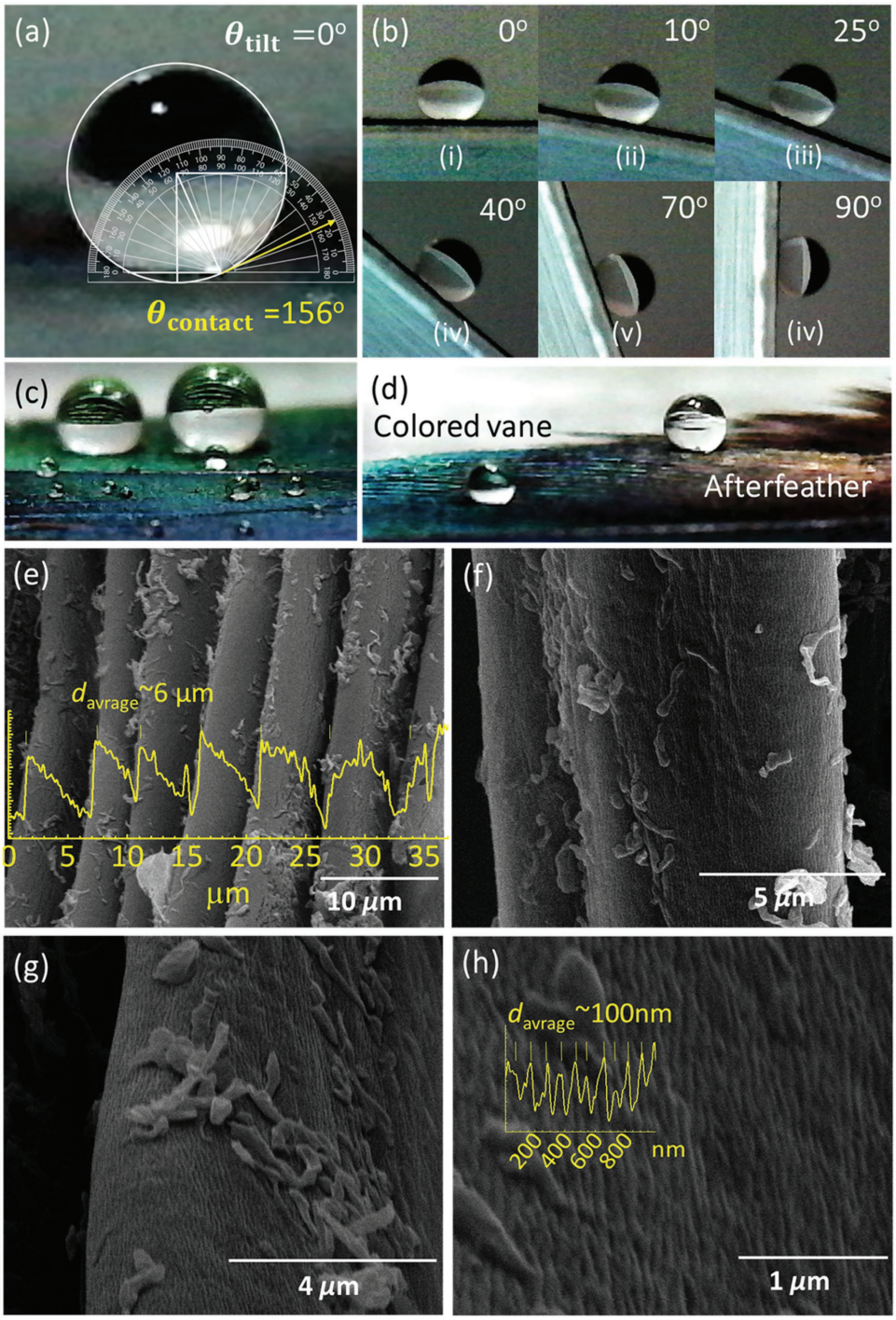

Figure 6. Contact angle measurements on a feather of Nicobar pigeon. a) A water droplet (1 µL) having a contact angle of 156° at the vane of the feather. b) Feather holds the water droplet when rotated such that gravity pulls the droplet opposite to the direction of growth of the barbules. c) Different sizes of water droplets sprinkled on the feather. d) Two droplets cast on the colored vane and afterfeather showing the superhydrophobicity of the feathers across its entire length. e–h) SEM images of the top surface of the Nicobar's feather. Feathers feature a periodic having an average interspacing of ≈6 µm. Nanoscale texturing has a periodicity of ≈100 nm. Such texturing enhances the hydrophobicity of the feathers.

in optical spectra was measured with increasing glucose concentrations. Two linear sensing regions have been defined in low and high concentration regimes. We anticipate that the underlying mechanism of light diffraction can provide a deeper understanding of structural coloration in Nicobar pigeon and provide design criteria for engineering applications in wavelength-selective filters, sensors, and nanophotonic devices.

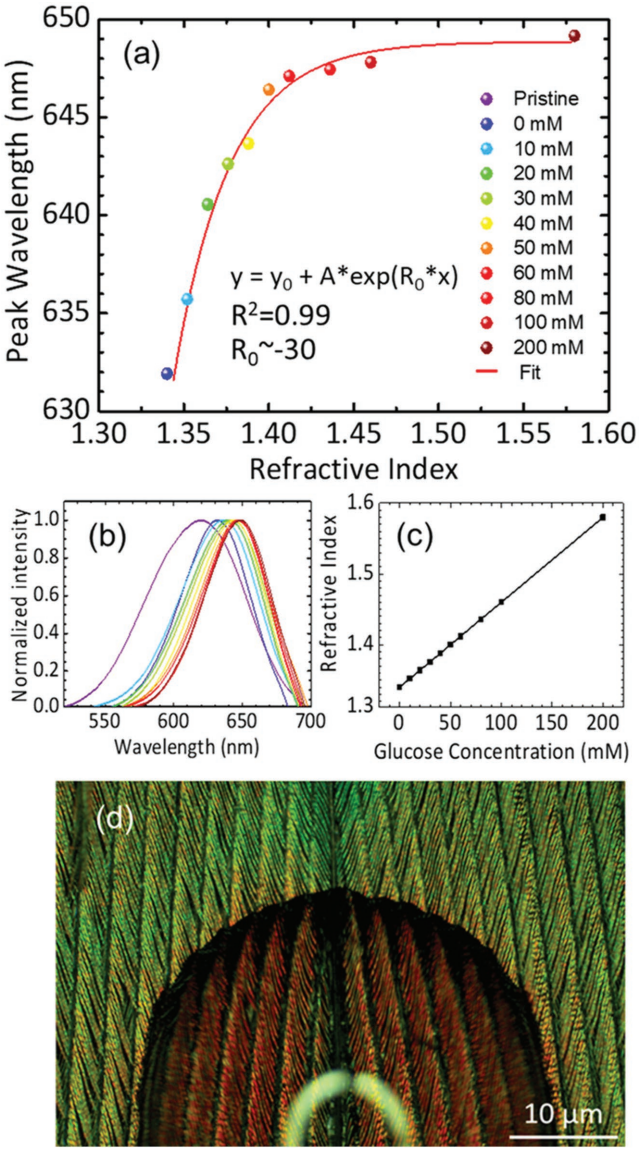

Figure 7. Refractive index sensing with Nicobar pigeon's feather. a) Measurement of glucose concentrations from 0 to 200 × 10^{-3} M. b) Spectral shift with increasing glucose concentration. c) Variation of the refractive index with increasing glucose concentration. d) Visual illustration of glucose sensing under an optical microscope. The feather surface undergoes a redshift upon pouring the glucose solution. The pristine region is unchanged.

4. Experimental Section

Optical microscopy (Zeiss, 5–100 ×) was carried out mainly on two kinds of feathers, both of which show predominantly two alternating colors: a RG and a GB when viewed at different angles. Calami of feathers were placed on glass slides to bring reasonable numbers of barbs (thereby barbules) in the horizontal plane in order to enhance their simultaneous visibility under the microscope. Bright field (BF) and dark field (DF) microscopy were used to visualize both feathers. Optical response of feathers at different angles was characterized using Ocean Optics (DH-2000) spectrometer in standard and in-house developed setups. Field emission scanning electron microscopy was used to visualize the surface of the feathers from different locations. The sessile drop method was used to measure the contact angle of the liquid on the feather's surface.

Supporting Information

Supporting Information is available from the Wiley Online Library or from the author.

Acknowledgements

The authors acknowledge Welcome Trust for the research funding.

Conflict of Interest

The authors declare no conflict of interest.

Keywords

coloration, diffraction, photonic structures, refractive index, scattering

[1] R. T. Gunther, *Robert Hooke – Micrographia, 1665*, Early Science in Oxford: Life and work of Robert Hooke, pt. 5, Printed for the Oxford Historical Society at the Clarendon Press, **1938**.
[2] Z. Han, Z. Mu, B. Li, Z. Wang, J. Zhang, S. Niu, L. Ren, *ACS Nano* **2016**, *10*, 8591.
[3] E. C. Regan, Y. Shen, J. J. Lopez, C. W. Hsu, B. Zhen, J. D. Joannopoulos, M. Soljačić, *ACS Photonics* **2016**, *3*, 532.
[4] Q. Yang, S. Zhu, W. Peng, C. Yin, W. Wang, J. Gu, W. Zhang, J. Ma, T. Deng, C. Feng, *ACS Nano* **2013**, *7*, 4911.
[5] D. Stavenga, S. Stowe, K. Siebke, J. Zeil, K. Arikawa, *Proc. R. Soc. London, Ser. B* **2004**, *271*, 1577.
[6] H. Onslow, *Nature* **1920**, *106*, 181.
[7] A. E. Seago, P. Brady, J.-P. Vigneron, T. D. Schultz, *J. R. Soc. Interface* **2009**, *6*, S165.
[8] S. Kinoshita, S. Yoshioka, J. Miyazaki, *Rep. Prog. Phys.* **2008**, *71*, 076401.
[9] P. Vukusic, R. Wootton, J. Sambles, *Proc. R. Soc. London, Ser. B* **2004**, *271*, 595.
[10] H. Butt, A. K. Yetisen, D. Mistry, S. A. Khan, M. U. Hassan, S. H. Yun, *Adv. Opt. Mater.* **2016**, *4*, 489.
[11] V. Sharma, M. Crne, J. O. Park, M. Srinivasarao, *Science* **2009**, *325*, 449.
[12] P. Vukusic, D. Stavenga, *J. R. Soc. Interface* **2009**, *6*, S133.
[13] J. Lythgoe, J. Shand, *J. Exp. Biol.* **1989**, *141*, 313.
[14] D. J. Brink, N. G. van der Berg, A. J. Botha, *Appl. Opt.* **2002**, *41*, 717.
[15] A. R. Parker, *J. Exp. Biol.* **1998**, *201*, 2343.
[16] M. Amiri, H. M. Shaheen, *Micron* **2012**, *43*, 159.
[17] C. J. Chandler, B. D. Wilts, S. Vignolini, J. Brodie, U. Steiner, P. J. Rudall, B. J. Glover, T. Gregory, R. H. Walker, *Sci. Rep.* **2015**, *5*, 11645.
[18] A. Levy-Lior, E. Shimoni, O. Schwartz, E. Gavish-Regev, D. Oron, G. Oxford, S. Weiner, L. Addadi, *Adv. Funct. Mater.* **2010**, *20*, 320.

[19] L. Bai, Z. Xie, W. Wang, C. Yuan, Y. Zhao, Z. Mu, Q. Zhong, Z. Gu, *ACS Nano* **2014**, *8*, 11094.
[20] R. Merindol, S. Diabang, O. Felix, T. Roland, C. Gauthier, G. Decher, *ACS Nano* **2015**, *9*, 1127.
[21] B. J. Glover, H. M. Whitney, *Ann. Bot.* **2010**, *105*, 505.
[22] C. Hébant, D. W. Lee, *Am. J. Bot.* **1984**, *71*, 216.
[23] S. Vignolini, P. J. Rudall, A. V. Rowland, A. Reed, E. Moyroud, R. B. Faden, J. J. Baumberg, B. J. Glover, U. Steiner, *Proc. Natl. Acad. Sci. USA* **2012**, *109*, 15712.
[24] S. Vignolini, B. Glover, U. Steiner, *Biomimetics in Photonics*, Taylor & Francis, London **2012**, p. 1.
[25] P. V. Braun, *Nature* **2011**, *472*, 423.
[26] D. G. Stavenga, H. L. Leertouwer, N. J. Marshall, D. Osorio, *Proc. R. Soc. London, Ser. B* **2010**, *278*, 2098.
[27] J. Remsen Jr., *J. Field Ornithol.* **2015**, *86*, 182.
[28] D. G. Stavenga, *Mater. Today Proc.* **2014**, *1*, 109.
[29] Y. Liu, X. Chen, J. Xin, *Bioinspiration Biomimetics* **2008**, *3*, 046007.
[30] C. M. Eliason, M. D. Shawkey, *J. R. Soc. Interface* **2012**, *9*, 2279.
[31] D. Steadman, *J. Biogeogr.* **1997**, *24*, 737.
[32] S. Leclaire, P. Pierret, M. Chatelain, J. Gasparini, *Behav. Ecol.* **2014**, *25*, 1192.
[33] H. Yin, L. Shi, J. Sha, Y. Li, Y. Qin, B. Dong, S. Meyer, X. Liu, L. Zhao, J. Zi, *Phys. Rev. E* **2006**, *74*, 051916.
[34] J. Sun, B. Bhushan, J. Tong, *RSC Adv.* **2013**, *3*, 14862.
[35] S. M. Doucet, M. D. Shawkey, G. E. Hill, R. Montgomerie, *J. Exp. Biol.* **2006**, *209*, 380.
[36] S. Yoshioka, S. Kinoshita, *Forma* **2002**, *17*, 169.
[37] C. H. Greenewalt, W. Brandt, D. D. Friel, *J. Opt. Soc. Am.* **1960**, *50*, 1005.
[38] K. Liu, L. Jiang, *ACS Nano* **2011**, *5*, 6786.
[39] M. Xiao, Y. Li, M. C. Allen, D. D. Deheyn, X. Yue, J. Zhao, N. C. Gianneschi, M. D. Shawkey, A. Dhinojwala, *ACS Nano* **2015**, *9*, 5454.
[40] K. Liu, L. Jiang, *Nano Today* **2011**, *6*, 155.
[41] X. Wang, B. Ding, J. Yu, M. Wang, *Nano Today* **2011**, *6*, 510.
[42] X. Zhang, Z. Li, K. Liu, L. Jiang, *Adv. Funct. Mater.* **2013**, *23*, 2881.
[43] S. Zhang, Y. Chen, *Sci. Rep.* **2015**, *5*, 8441.
[44] L. Meylan, S. Susstrunk, *Proc. SPIE* **2004**, *5292*, 46.
[45] J. Huang, X. Wang, Z. L. Wang, *Nanotechnology* **2007**, *19*, 025602.
[46] C. P. Tsangarides, A. K. Yetisen, F. da Cruz Vasconcellos, Y. Montelongo, M. M. Qasim, T. D. Wilkinson, C. R. Lowe, H. Butt, *RSC Adv.* **2014**, *4*, 10454.
[47] X. Yang, J. Zhu, L. Qiu, D. Li, *Adv. Mater.* **2011**, *23*, 2833.
[48] A. K. Yetisen, H. Qu, A. Manbachi, H. Butt, M. R. Dokmeci, J. P. Hinestroza, M. Skorobogatiy, A. Khademhosseini, S. H. Yun, *ACS Nano* **2016**, *10*, 3042.
[49] X. Li, W.-C. Chang, Y. J. Chao, R. Wang, M. Chang, *Nano Lett.* **2004**, *4*, 613.
[50] A. K. Yetisen, A. F. Coskun, G. England, S. Cho, H. Butt, J. Hurwitz, M. Kolle, A. Khademhosseini, A. J. Hart, A. Folch, *Adv. Mater.* **2015**, *28*, 1724.
[51] K. ul Hasan, M. H. Asif, M. U. Hassan, M. O. Sandberg, O. Nur, M. Willander, S. Fagerholm, P. Strålfors, *Electrochim. Acta* **2015**, *174*, 574.
[52] A. K. Yetisen, H. Butt, L. R. Volpatti, I. Pavlichenko, M. Humar, S. J. Kwok, H. Koo, K. S. Kim, I. Naydenova, A. Khademhosseini, *Biotechnol. Adv.* **2016**, *34*, 250.
[53] N. M. Farandos, A. K. Yetisen, M. J. Monteiro, C. R. Lowe, S. H. Yun, *Adv. Healthcare Mater.* **2015**, *4*, 792.
[54] R. Riedler, C. Pesme, J. Druzik, M. Gleeson, E. Pearlstein, *J. Am. Inst. Conserv.* **2014**, *53*, 44.
[55] M. Xiao, A. Dhinojwala, M. Shawkey, *Opt. Express* **2014**, *22*, 14625.